Design and Spectroscopic Characterization of Peptide Models for the Plastocyanin Copper-Binding Loop

ARTICLE *in* INORGANIC CHEMISTRY · JUNE 2002

Impact Factor: 4.76 · DOI: 10.1021/ic010555a · Source: PubMed

4 AUTHORS, INCLUDING:

Brian R Gibney
City University of New York - Brooklyn College
78 PUBLICATIONS **2,928** CITATIONS
SEE PROFILE

Victoria J DeRose
University of Oregon
82 PUBLICATIONS **2,776** CITATIONS
SEE PROFILE

Volume 41
Number 10
May 20, 2002

Inorganic Chemistry
including bioinorganic chemistry

Design and Spectroscopic Characterization of Peptide Models for the Plastocyanin Copper-Binding Loop

Roxanne G. Daugherty,[†] Tomasz Wasowicz,[†,‡] Brian R. Gibney,[§] and Victoria J. DeRose*,[†]

Department of Chemistry, Texas A&M University, College Station, Texas 77842-3012, and Department of Chemistry, Columbia University, New York, New York 10027

Received May 29, 2001

The Cu(II)- and Co(II)-binding properties of two peptides, designed on the basis of the active site sequence and structure of the blue copper protein plastocyanin, are explored. Peptide BCP-A, Ac-Trp-$(Gly)_3$-Ser-Tyr-Cys-Ser-Pro-His-Gln-Gly-Ala-Gly-Met-$(Gly)_3$-His-$(Gly)_2$-Lys-$CONH_2$, conserves the Cu-binding loop of plastocyanin containing three of the four copper ligands and has a flexible $(Gly)_3$ linker to the second His ligand. Peptide BCP-B, Ac-Trp-$(Gly)_3$-Cys-Gly-His-Gly-Val-Pro-Ser-His-Gly-Met-Gly-$CONH_2$, contains all four blue copper ligands, with two on either side of a β-turn. Both peptides form 1:1 complexes with Cu(II) through His and Cys ligands. BCP-A, the ligand loop, binds to Cu(II) in a tetrahedrally distorted square plane with axial solvent ligation, while BCP-B–Cu(II) has no tetrahedral distortion in aqueous solution. In methanolic solution, distortion of the square plane is evident for both BCP–Cu(II) complexes. Tetrahedral Co(II) complexes are observed for both peptides in aqueous solution but with 4:2 peptide:Co(II) stoichiometries as estimated by ultracentrifugation. Cu(II) reduction potentials for the aqueous peptide–Cu(II) complexes were measured to be $+75 \pm 30$ mV vs NHE for BCP-A–Cu(II) and -10 ± 20 mV vs NHE for BCP-B–Cu(II). The results indicate that the plastocyanin ligand loop can act as a metal-binding site with His and Cys ligands in the absence of the remainder of the folded protein but, by itself, cannot stabilize a type 1 copper site, emphasizing the role of the protein matrix in protecting the Cu binding site from solvent exposure and the Cys from oxidation.

Introduction

Understanding the unique properties of metal sites in proteins has been the target of extensive structural, spectroscopic, and modeling studies. The design of metal-binding peptides to mimic metalloprotein active sites is an appealing approach, allowing one to probe the minimum amount of the protein necessary to create a unique coordination environment. In the most direct approach, peptides are used to build synthetic analogues for known metalloprotein active sites. Models for zinc-finger proteins,[1,2] cytochromes,[3−5] ferredoxin and high potential iron protein sites,[4,6] Ca(II) binding domains,[7] the zinc site in carbonic anhydrase,[8] and the structural zinc site in alcohol dehydrogenase[9] have been reported.

Blue copper proteins have long held the interest of bioinorganic chemists due to their interesting spectroscopic

* Corresponding author. Phone: 979-862-1401. Fax: 979-845-4719. E-mail: derose@mail.chem.tamu.edu.
[†] Texas A&M University.
[‡] On leave from the Institute of Nuclear Chemistry and Technology, Dorodna 16, 03-195 Warsaw, Poland. Present address: Department of Physics and Astronomy, Georgia State University, Atlanta, GA 30303.
[§] Columbia University.

(1) Berg, J. M.; Godwin, H. A. *Annu. Rev. Biophys. Biomol. Struct.* **1997**, *26*, 357−371.
(2) Chen, X.; Chi, M.; Giedroc, D. P. *J. Biol. Inorg. Chem.* **2000**, *5*, 93−101.
(3) DeGrado, W. F.; Wasserman, Z. R.; Lear, J. D. *Science* **1989**, *243*, 622−628.
(4) Gibney, B. R.; Mulholland, S. E.; Rabanal, F.; Dutton, P. L. *Proc. Natl. Acad. Sci. U.S.A.* **1996**, 93, 15041−15046.
(5) Benson, D. R.; Hart, B. R.; Zhu, X.; Doughty, M. B. *J. Am. Chem. Soc.* **1995**, *117*, 8502−8510.
(6) Mulholland, S. E.; Gibney, B. R.; Rabanal, F.; Dutton, P. L. *J. Am. Chem. Soc.* **1998**, *120*, 10296−10302.
(7) Prorok, M.; Warder, S. E.; Blandl, T.; Castellino, F. J. *Biochemistry* **1996**, *35*, 16528−16534.

10.1021/ic010555a CCC: $22.00
Published on Web 04/19/2002

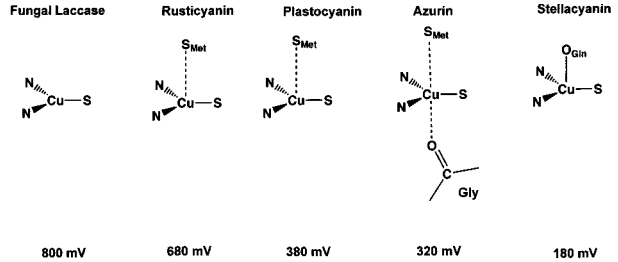

Figure 1. Cu(II) coordination environment and approximate midpoint reduction potentials, E_m, of selected blue copper proteins. As axial interactions with the Cu(II) are increased, E_m decreases.[14]

properties and the challenges of synthesizing inorganic model complexes that mimic the spectroscopic and redox properties of the blue copper site. Natural blue copper, or type I copper, proteins have been extensively studied both spectroscopically and structurally.[10−14] Blue copper proteins are characterized by their intense blue color, originating from a sulfur to Cu(II) LMCT band around 600 nm, with extinction coefficients between 2500 and 6000 M^{-1} cm^{-1}, small ^{63,65}Cu(II) parallel hyperfine coupling constants ($A_{\|} \sim (60-90) \times 10^{-4}$ cm^{-1}), and positive Cu(II) reduction potentials ranging from +150 to +800 mV vs NHE.[11,12] The Cu(II) ion in this site is bound in a distorted, or flattened, tetrahedral active site that includes two histidines and a cysteine in a trigonal plane.[10,14] Axial interactions differ among blue copper proteins. Plastocyanin has a Met thioether axial ligand, and in azurin, a backbone carbonyl oxygen acts as a weak fifth ligand opposite the Met. In stellacyanin, Met is replaced by a Gln that coordinates to the copper ion via the amide oxygen, and in laccase Cu(II) sites, there are no axial interactions of the protein with the copper ion.[11] The axial interactions are important in tuning the reduction potential of the Cu(II) in the active site.[13,14] As shown in Figure 1, increased axial interactions of the protein with the Cu(II) result in the decrease of the Cu(II) reduction potential.

Design of inorganic model complexes for the blue copper site has proven to be a challenging endeavor that began in 1963 when Broman and Malmström showed that the blue copper site contained a Cu(II) ion.[15] Kitajima and co-workers reported the first spectroscopic model complex for a blue copper site in 1990,[16,17] and since then only Tolman and co-workers have succeeded in creating other model complexes that mimic the structural and spectroscopic features of the blue copper site.[18,19] The unique spectroscopic and redox properties and difficulty in synthesis of a model for the type 1 site have led to the hypothesis that the protein matrix imposes strain on the Cu(II) ion by creating a rack or entatic state not yielding to the geometric preferences of the Cu(II) ion.[20]

Ryde and co-workers have questioned the entatic state model for blue Cu sites on the basis of results of theoretical calculations that predicted that a small molecule model for the blue site, $[Cu(im)_2SCH_3S(CH_3)_2]^+$, adopts a low-energy structure very similar to that of the protein.[21,22] This would suggest that a blue Cu site might be formed if Cu(II) were presented with the appropriate amino acid ligands. Even so, Hellinga found the type I site to be elusive in attempts to engineer a blue copper protein using the design algorithm DEZYMER and the nonnative host protein thioredoxin.[23] Cys thiolate oxidation and competing protein or solvent ligands were problematic, and the closest approach was a tetrahedral type 1.5 site consisting of 2 His, 1 Cys, and a strong exogeneous ligand, N_3^-.[23] Conversely, it has recently been reported that "transplanting" Cu-binding loops of several blue Cu proteins to a cupredoxin-fold scaffold from amicyanin results in type 1 sites in all cases.[24] These and other studies point to critical elements in the native blue copper proteins that play important roles in shielding Cys from oxidation and protecting Cu(II) from solvent.

One way to investigate the biophysical interactions of the protein that are responsible for the stabilization of a unique inorganic Cu(II) site is to design metallopeptides based upon the blue copper site. Previous attempts at metallopeptide design of a blue copper site, including a linear peptide,[25] a cyclic peptide,[26] and a 3-α-helix bundle,[27] have met with limited success, most likely due to the inability to control redox chemistry between the Cys and Cu(II) ion. Wittung-Stafshede and co-workers have shown that addition of Cu(II) to a peptide analogous to the azurin ligand loop triggers β-hairpin formation, but this peptide containing the Cys, one His, and Met ligands does not result in blue copper site formation.[28] Haehnal and co-workers have recently re-

(8) Herr, U.; Spahl, W.; Trojandt, G.; Steglich, W.; Thalser, F.; van Eldik, R. *Bioorg. Med. Chem.* **1999**, *7*, 699−707.
(9) Bergman, T.; Jörnvall, H.; Holmquist, B.; Vallee, B. G. *Eur. J. Biochem.* **1992**, *205*, 467−470.
(10) (a) Guss, J. M.; Freeman, H. C. *J. Mol. Biol.* **1983**, *169*, 521−563. (b) Guss, J. M.; Bartunik, H. D.; Freeman, H. C. *Acta Crystallogr. B* **1992**, *48*, 790−811. (c) Guss, J. M.; Harrowell, P. R.; Murata, M.; Noris, V. A.; Freeman, H. C. *J. Mol. Biol.* **1986**, *192*, 361−387.
(11) Holm, R. H.; Kennepohl, P.; Solomon, E. I. *Chem. Rev.* **1996**, *96*, 2239−2314.
(12) Solomon, E. I.; LaCroix, L. B.; Randall, D. W. *Pure Appl. Chem.* **1998**, *70*, 799−808.
(13) Solomon, E. I.; Lowery, M. D.; Guckert, J. A.; LaCroix, L. B. *Adv. Inorg. Chem.* **1997**, *253*, 317−330.
(14) (a) Malström, B. G.; Wittung-Stafshede, P. *Coord. Chem. Rev.* **1999**, *185*−*186*, 127−140. (b) Gray, H. B.; Malström, B. G.; Williams, R. J. P. *J. Biol. Inorg. Chem.* **2000**, *5*, 551−559.
(15) (a) Broman, L.; Malström, B. G.; Aasa, R.; Vänngård, T. *Biochim. Biophys. Acta* **1963**, *75*, 365−376. (b) Malström, B. G. *Eur. J. Biochem.* **1994**, *223*, 711−718.
(16) Kitajima, N.; Fujisawa, K.; Moro-oka, Y. *J. Am. Chem. Soc.* **1990**, *112*, 3210−3212.
(17) Kitajima, N.; Fujisawa, K.; Tanaka, M.; Moro-oka, Y. *J. Am. Chem. Soc.* **1992**, *114*, 9232−9233.
(18) Holland, P. L.; Tolman, W. B. *J. Am. Chem. Soc.* **1999**, *121*, 7270−7271.
(19) Holland, P. L.; Tolman, W. B. *J. Am. Chem. Soc.* **2000**, *122*, 6331−6332.
(20) Gray, H. B.; Malström, B. G. *Comments Inorg. Chem.* **1983**, *2*, 203−209.
(21) Ryde, U.; Olsson, M. H. M.; Pierloot, K.; Roos, B. O. *J. Mol. Biol.* **1996**, *261*, 586−596.
(22) DeKerpel, J. O.; Ryde, U. *Proteins* **1999**, *36*, 157−174.
(23) Hellinga, H. W. *J. Am. Chem. Soc.* **1998**, *120*, 10055−10066.
(24) Bunning, C.; Canters, G. W.; Comba, P.; Dennison, C.; Jeuken, L.; Melter, M.; Sanders-Loehr, J. *J. Am. Chem. Soc.* **2000**, *122*, 204−211.
(25) Zaima, H.; Ueyama, N.; Nakamura, A.; Aimoto, S. *Chem. Lett.* **1993**, *11*, 1885−1888.
(26) Fatturusso, R.; Morelli, G.; Lombardi, A.; Nastri, F.; Maglio, O.; D'Auria, G.; Pedone, C.; Pavone, V. *Biopolymers* **1995**, *37*, 401−410.
(27) Lombardi, A.; Bryson, J. W.; DeGrado, W. F. *Biopolymers* **1996**, *40*, 495−504.

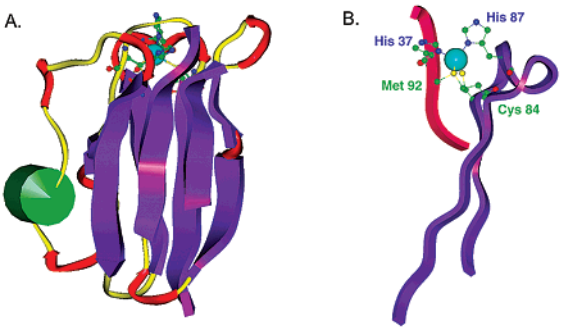

C. *Tyr*^{80} *Ser Phe Tyr* ***Cys***^{84} *Ser Pro* ***His***^{87} *Gln Gly Ala Gly* ***Met***^{92} *Val Gly Lys*^{95}

Figure 2. (A) Ribbon diagram of Poplar plastocyanin (PDB code 1PLC[10]) showing the Cu binding site at the top of the β-barrel cupredoxin fold. Copper ligands are shown in ball-and-stick rendering. (B) View of PLC active site including residues 79−99 (purple) and 35−50 (red). Note that three of the four ligands are contained within nine residues of the N-terminal β-sheet. (C) Sequence of Poplar PLC ligand loop and surrounding residues. The loop is underlined and the ligands are in bold with the Poplar PLC residue number denoted.

ported a library of templated 4-α-helix bundles, a number of which bind Cu(II) in type 2 coordination with an observable thiolate−copper(II) LMCT.[29] One of the templated proteins is stable for up to 15 min after addition of Cu(II). It is evident from these experiments that the copper(II)−thiolate redox chemistry is one major roadblock to synthesis of a stable blue copper metallopeptide.

Herein we report two copper(II) binding peptides designed to address the requirements of the blue copper site. The copper(II)−thiolate redox chemistry is controlled and copper(II)−peptide complexes are formed in aqueous solution under inert atmosphere. A β-hairpin with the four blue copper ligands results in an aqueous tetragonal copper(II) complex, while a peptide containing the ligand loop sequence from poplar plastocyanin with an added His results in a copper(II)−peptide complex with some tetrahedral twist in the square plane. The spectroscopic characterization, stoichiometry, and reduction potentials are described for these copper(II)−peptide complexes. The results are used to deduce proposed coordination environments and to compare the copper(II)−peptide complexes with the blue copper proteins.

Results

Peptide Design. A general feature of blue copper proteins that is provocative for a peptide model is the ligand loop, which is located near the C-terminus of the protein. In Poplar plastocyanin (PLC), the ligand loop encompasses the Cys, Met, and His ligands within 9 residues, Cys84, His87, and Met92.[10] The second histidine ligand, His37, is distant in linear sequence and brought to the active site by the protein fold (Figure 2).[10]

The first designed peptide, denoted BCP-A, conserves the ligand binding loop residues corresponding to Poplar PLC Tyr83-Met92 (Figure 2).[10b] Flexible $(Gly)_x$ linkers were

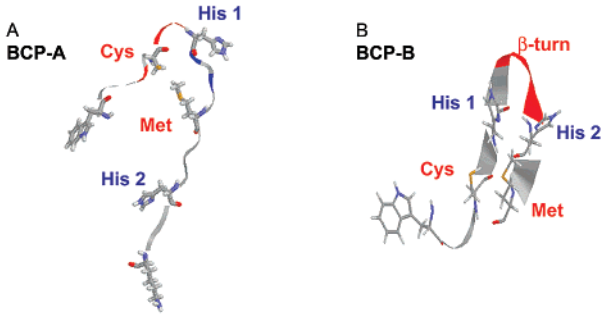

BCP-A
Trp $(Gly)_3$ *Ser Tyr* ***Cys*** *Ser Pro* ***His*** *Gln Gly Ala Gly* ***Met*** $(Gly)_3$ ***His*** $(Gly)_2$ *Lys*

BCP-B
Trp $(Gly)_3$ ***Cys*** *Gly* ***His*** *Gly Val Pro Ser* ***His*** *Gly* ***Met*** *Gly*

Figure 3. Energy-minimized molecular models and sequences of (A) BCP-A and (B) BCP-B. Ligand residues and terminal residues are shown in stick representation in the models; ligands are bold in the sequences. (A) PLC ligand loop is underlined in BCP-A; (B) β-turn initiating sequence is underlined in BCP-B.

added outside the ligand loop to connect a second His C-terminal to the Met residue. An N-terminal Trp and a C-terminal Lys were included for spectroscopic detection and for enhancement of solubility, respectively. Peptide structures calculated using molecular mechanics were used to guide the choice of the number of Gly residues (see Materials and Methods). The energy-minimized structure of the selected BCP-A sequence is shown in Figure 3A.

A second peptide, BCP-B, was designed to conserve only the presence of a β-turn in the ligand region between the His87 and Met92 of Poplar PLC. The blue copper ligands, His_2, Cys, and Met, were added about the β-turn sequence of *Val-Pro-Ser-His*, based upon a type II β-turn nucleating sequence of *Val-Pro-*^{D}*Ser-His* reported by Imperiali and Kapoor.[30] The BCP-B sequence was designed such that on either side of the β-turn one nitrogen- and one sulfur-containing ligand were presented to the metal. Glycines were placed between the ligand residues to allow formation of a compact binding site without steric interference from an amino acid side chain. The sequence and energy-minimized structure of the BCP-B β-hairpin are presented in Figure 3B.

Copper Coordination in Aqueous Solution. Complexes of Cu(II) and thiolate-containing ligands are difficult to form in high yield in aqueous solution due to the oxidation by Cu(II) of thiolates to disulfides. Reactions of BCP-A and BCP-B with Cu(II) at neutral pH suffered from 80 to 95% oxidation of the cysteine residue to disulfides, resulting in a peptide dimer with Cu(I) or disproportionated Cu(II) in solution. Previous work by Davis et al. reported copper(II)−thiolate complexes produced in about 40% yield at pH 10 in an NH_3-containing solution.[31] The high pH causes deprotonation of the cysteine and increases its ligand propensity, whereas the coordinating NH_3 apparently protects Cu(II) from precipitation and reduction. At pH 9.8 in the NH_3-containing buffer, BCP-A formed Cu(II) complexes in about

(28) Pozdnyaokava, I.; Guidry, J.; Wittung-Stafshede, P. *J. Am. Chem. Soc.* **2000**, *122*, 6337−6338.
(29) Schnepf, R.; Horth, P.; Bill, E.; Wieghardt, K.; Hildebrandt, P.; Haehnel, W. *J. Am. Chem. Soc.* **2001**, *123*, 2186−2195.
(30) Imperiali, B.; Kapoor, T. M. *Tetrahedron* **1993**, *49*, 3501−3510.
(31) Davis, F. J.; Gilbert, B. C.; Norman, R. O. C.; Symons, M. C. R. *J. Chem. Soc., Perkin Trans. 2* **1983**, 1763−1771.

Table 1. Spectroscopic and Redox Properties of Peptide Complexes with Cu(II) and Co(II)

peptide sample	λ (nm) (ϵ (M^{-1} cm^{-1})) LMCT	d−d	$g_{\|\|}$, $A_{\|\|}{}^c$ (10^{-4} cm^{-1})	$A(^1H)^d$ (MHz)	$E^{1/2}$ (mV vs NHE)
BCP-A−Cu(II), pH 9.8	335 (1750)	550 (220)	2.18, 190	2.4, 4.9. 8.5, 19	+75 ± 30
BCP-A−Cu(II) MeOH[a]	410 (1300)	600 (100)			
BCP-A−Cu(II) MeOH	430 (550)	600 (60)			
BCP-A−Co(II)[b]	310 (1160)	625 (230)			
BCP-B−Cu(II), pH 9.8	345 (4200)	550 (30)	2.16, 180	2.5, 4.2, 5.0, 7.8, 20	−10 ± 20
BCP-B−Cu(II) MeOH[a]	360 (1700)	560 (170)			
BCP-B−Cu(II) MeOH	390 (700)	590 (80)			
BCP-B−Co(II)[b]	310 (1330)	625 (290)			

[a] Peptides deprotonated with $NaOCH_3$. [b] Tetrahedral 4:2 BCP:Co(II) complexes in pH 7.5 HEPES buffer. [c] X-band EPR parameters. [d] Hyperfine couplings measured by Q-band ENDOR at $g_{||}$ position of EPR spectra

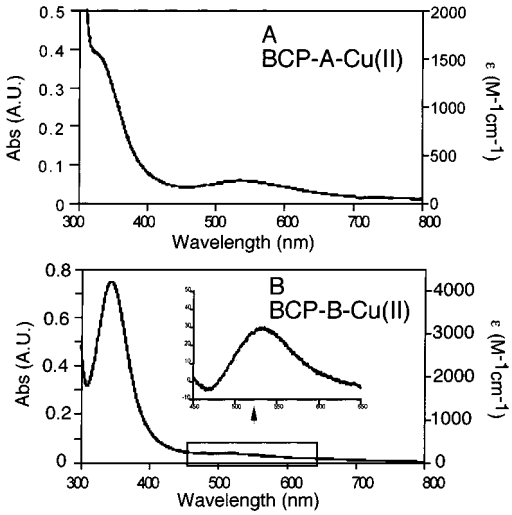

Figure 4. UV−visible absorption spectra for (A) BCP-A and (B) BCP-B. The left axis is in absorbance units, and the right axis is in units of extinction coefficient. The inset shows a blowup of the d−d region from 450 to 650 nm (ϵ vs λ).

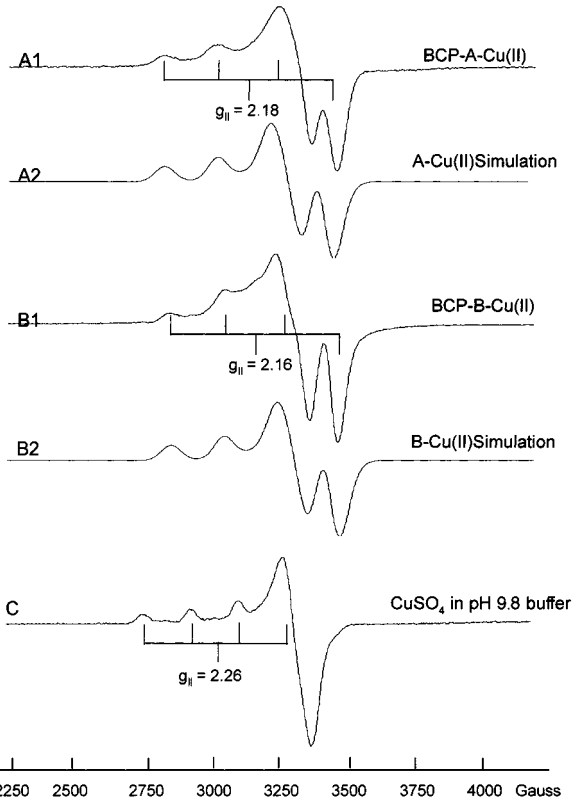

Figure 5. X-band EPR spectrum (A1) and simulation (A2) for BCP-A−Cu(II): $g_\perp = 2.05$; $g_{||} = 2.18$; $A_{||} = 195 \times 10^{-4}$ cm^{-1}. EPR spectrum (B1) and simulation (B2) for BCP-B−Cu(II): $g_\perp = 2.05$; $g_{||} = 2.16$; $A_{||} = 188 \times 10^{-4}$ cm^{-1}. (C) EPR spectrum of $CuSO_4$ in pH 9.8 buffer solution: $g_\perp = 2.06$; $g_{||} = 2.26$; $A_{||} = 177 \times 10^{-4}$ cm^{-1}. All spectra were measured at 2 mW microwave power, 8 G modulation amplitude, 10 K, and 9.4 GHz.

50% yield upon addition of 1 equiv of $CuSO_4$, while BCP-B consistently showed a slightly higher yield of 60−65%.

The UV−visible spectra of the aqueous BCP−Cu(II) complexes are shown in Figure 4 , and the spectroscopic parameters for the complexes are summarized in Table 1. The BCP−Cu(II) complexes display similar UV−visible spectra, with thiolate → Cu(II) LMCT bands at 335 nm ($\epsilon \sim 1500-1700$ M^{-1} cm^{-1}) for BCP-A−Cu(II) and 345 nm ($\epsilon \sim 4200$ M^{-1} cm^{-1}) for BCP-B−Cu(II). Both BCP-A−Cu(II) and BCP-B−Cu(II) display a d−d band at 550 nm, but with an extinction coefficient of $\epsilon \sim 220$ M^{-1} cm^{-1}, the BCP-A−Cu(II) d−d band is much more intense than that of BCP-B−Cu(II), which has $\epsilon \sim 30$ M^{-1} cm^{-1}. The 220 M^{-1} cm^{-1} ϵ_{d-d} value for BCP-A−Cu(II) is larger than expected for the parity forbidden transition associated with a Jahn−Teller distorted octahedral complex, which is typically no larger than about 50 M^{-1} cm^{-1}.[32,33] This increase in ϵ_{d-d} has recently been observed by Comba and co-workers in CuN_4 complexes that were shown by X-ray crystallography to have tetrahedral twists of the square plane[34] and could be the result of a similar mechanism in BCP-A−Cu(II).

EPR Spectroscopy. X-band EPR spectra and simulations of the BCP-A and BCP-B complexes with Cu(II), $S = {}^1/_2$, $I = {}^3/_2$, are shown in Figure 5 in comparison with the EPR spectrum of $CuSO_4$ in the pH 9.8 buffer. The $g_{||}$ and $A_{||}$ values for both peptide−copper(II) complexes (Table 1, Figure 5) are within the range observed for an N_2SX coordination environment of the square plane in a type 2 copper or tetragonal Cu(II) geometry, where X = O, N, or S.[35] Both peptide Cu(II) complexes display $A_{||}$ values characteristic of tetragonal Cu(II) complexes (Table 1). However, this does

(32) Lever, A. B. P. *Inorganic Electronic Spectroscopy*; Elselvier: New York, 1968.
(33) Cotton, F. A. *Chemical Applications of Group Theory*; Wiley: New York, 1990.
(34) Comba, P. *Coord. Chem. Rev.* **2000**, *200−202*, 217−245.
(35) Peisach, J.; Blumberg, W. E. *Arch. Biochem. Biophys.* **1974**, *165*, 691−708.

not rule out the possibility of a small twist in the square plane resulting in differences in the ϵ_{d-d} value between the two peptide complexes. Factors that influence the $A_{||}$ value, such as planarity and covalency, can work in opposing directions resulting in little net change of the observed $A_{||}$. Complexes with tetrahedral twists of up to 45° have been reported to retain $A_{||}$ values of 180×10^{-4} cm^{-1} or greater.[34]

Q-Band ENDOR of Aqueous Complexes. Electron nuclear double resonance, ENDOR, was employed to help elucidate the Cu(II) ligand environment in the BCP complexes. ENDOR, or EPR-detected NMR, allows the detection of NMR-active nuclei within close proximity (~6 Å) of a paramagnetic center.[36,37] Several ENDOR studies have been reported on blue copper proteins at both X- and Q-band frequencies.[38−41] The higher magnetic fields associated with Q-band (35 GHz) ENDOR facilitate the separation of ^{1}H and ^{14}N resonances.

Figure 6 shows the ^{1}H ENDOR spectra of the BCP−Cu(II) complexes along with those of the reference samples copper tetraimidazole (Cu(imid)$_4$), $CuSO_4$ in the pH 9.8 NH_3 buffer, and $CuSO_4$ in H_2O. ENDOR measurements were recorded at $g_{||}$ and $g_\perp$. Protons coupled to Cu(II) show ν_+ and ν_- signals centered about ν_H and split by the hyperfine coupling constant, *A*. ENDOR features in the region expected for ^{14}N were observed but lacked sufficient resolution for analysis (data not shown).

The $g_\perp$ ENDOR spectra of BCP-A−Cu(II) and BCP-B−Cu(II) display weakly coupled protons with $A_{obs} \sim 2.4-2.5$ and 4.9−5.0 MHz (Figure 6A,B). These are nearly identical to the couplings observed at $g_\perp$ in Cu(imid)$_4$ (Figure 6C)[42] and therefore are tentatively assigned to the protons on the imidazole ring of bound His. Both BCP−Cu(II) complexes also display protons of moderate coupling, $A_{obs} = 8.5$ MHz for BCP-A−Cu(II) and 7.8−8.0 MHz for BCP-B−Cu(II). Protons of similar coupling are present in the $CuSO_4$−buffer sample at 7.1 MHz (Figure 6D) and are likely due to NH_3 or OH^- ligands, and in $CuSO_4$ in H_2O at 8.9 MHz due to coordination of water (Figure 6E). Since the BCP-A− and BCP-B−Cu(II) complexes have tetragonal geometries and are suspected to contain solvent ligands in the axial positions, the moderately coupled protons are likely from the non-peptide solvent ligands, NH_3, OH^- or H_2O.

The most unique ENDOR features displayed by natural blue copper proteins are strongly coupled protons with $A_H = 15-31$ MHz that arise from spin delocalization onto the cysteine β methylene protons.[40,41] These hyperfine couplings

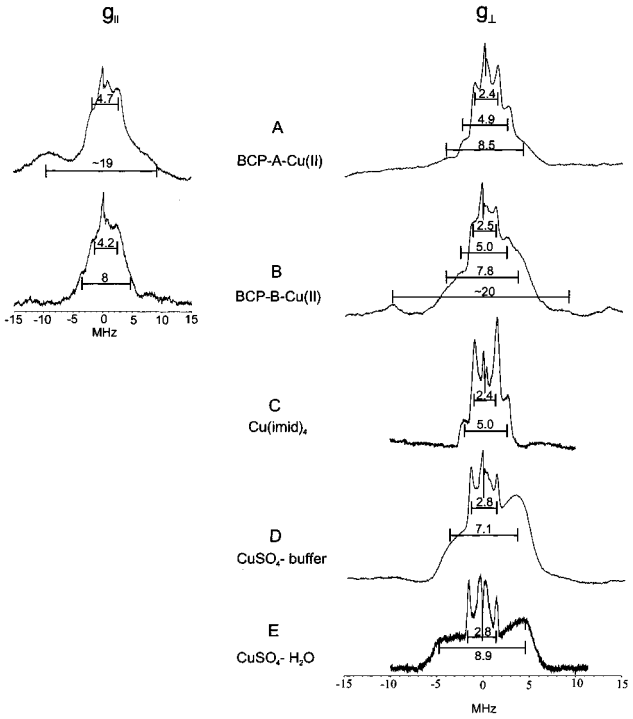

Figure 6. Q-band ^{1}H ENDOR spectra of Cu(II) complexes. ENDOR spectra of copper−peptide complexes were measured at both $g_\perp$ and $g_{||}$: (A) BCP-A−Cu(II), 1 mM, 120 scans, 20% glycerol; (B) BCP-B−Cu(II), 0.7 mM, 140 scans, 20% glycerol; (C) Cu(imid)$_4$, 1 mM, 15 scans, 60% glycerol; (D) $CuSO_4$ in pH 10 buffer, 0.6 mM, 10 scans, 20% glycerol; (E) $CuSO_4$ in H_2O, 1 mM, 15 scans, 60% glycerol. All spectra were recorded at 2 K, 34.1 GHz, with a scan rate of 0.5 MHz/s. Other parameters include the following: (A, B, D) 0.7 mW microwave power, 0.5 G modulation amplitude; (C) 2.25 mW microwave power, 0.7 G modulation amplitude; (E) 4.4 mW microwave power, 0.7 G modulation amplitude. Protons coupled to the Cu(II) show ν_+ and ν_- signals centered about ν_H and split by the observed hyperfine coupling constant, $A(^1H)$. Hyperfine couplings are indicated on each spectrum in MHz.

are sensitive to both the π spin density on the sulfur and the Cu−S−CH_2 dihedral angle.[40] Weak ^{1}H ENDOR signals were detected in the $g_\perp$ ENDOR spectrum of BCP-B at $A_H \sim 20$ MHz (Figure 6B), and in the $g_{||}$ spectrum of BCP-A at $A_H \sim 19$ MHz (Figure 6A). Because these signals are low intensity and not isotropic, they do not arise from the same spin delocalization mechanism as the strongly coupled protons in blue copper proteins. In the absence of the strong delocalization from the Cu(II) to the S_{Cys}, the β-CH_2 protons of the BCP−Cu(II) complexes will have weaker couplings than those in the blue copper proteins, and the signals are likely within the ~8 MHz ^{1}H ENDOR envelope.

Redox Potentiometry. The reduction potentials of the BCP−Cu(II) aqueous complexes were measured utilizing redox titrations monitoring the appearance or disappearance of the S−Cu(II) LMCT band at 335 and 345 nm for BCP-A−Cu(II) and BCP-B−Cu(II), respectively. The reductive titrations and corresponding Nernst curves are shown in Figure 7, and the average reduction potentials calculated from separate titrations are listed in Table 1. BCP-B−Cu(II) has a partially reversible (40−60% recovery of LMCT intensity) reduction with a midpoint of -10 ± 20 mV vs NHE. BCP-A−Cu(II) has a more positive reduction potential than BCP-B−Cu(II) of $+75 \pm 30$ mV. The ambient potential of the pH 9.8 buffer and mediators solution is near the mid-

(36) Hoffman, B. M.; DeRose, V. J.; Doan, P. E.; Gurbiel, R. J.; Houseman, A. L. P.; Telser, J. *Biol Magn. Reson.* **1993**, *13*, 151−218.
(37) DeRose, V. J.; Hoffman, B. M. *Methods Enzymol.* **1995**, *246*, 554−589.
(38) Robert, J. E.; Brown, T. G.; Hoffman, B. M.; Peisach, J. *J. Am. Chem. Soc.* **1980**, *102*, 825−829.
(39) Roberts, J. E.; Cline, J. F.; Lum, V.; Freeman, H. C.; Gray, H. B.; Peisach, J.; Reinhammer, B.; Hoffman, B. M. *J. Am. Chem. Soc.* **1984**, *106*, 5324−5330.
(40) Werst, M. W.; Davoust, C. E.; Hoffman, B. M. *J. Am. Chem. Soc.* **1991**, *113*, 1533−1538.
(41) Veselov, A.; Olesen, K.; Sienkewicz, A.; Shapleigh, J. P.; Scholes, C. P. *Biochemistry* **1998**, *37*, 6095−6105.
(42) Van Camp, H. L.; Sands, R. H.; Fee, J. A. *J. Chem. Phys.* **1981**, *75*, 2098−2107.

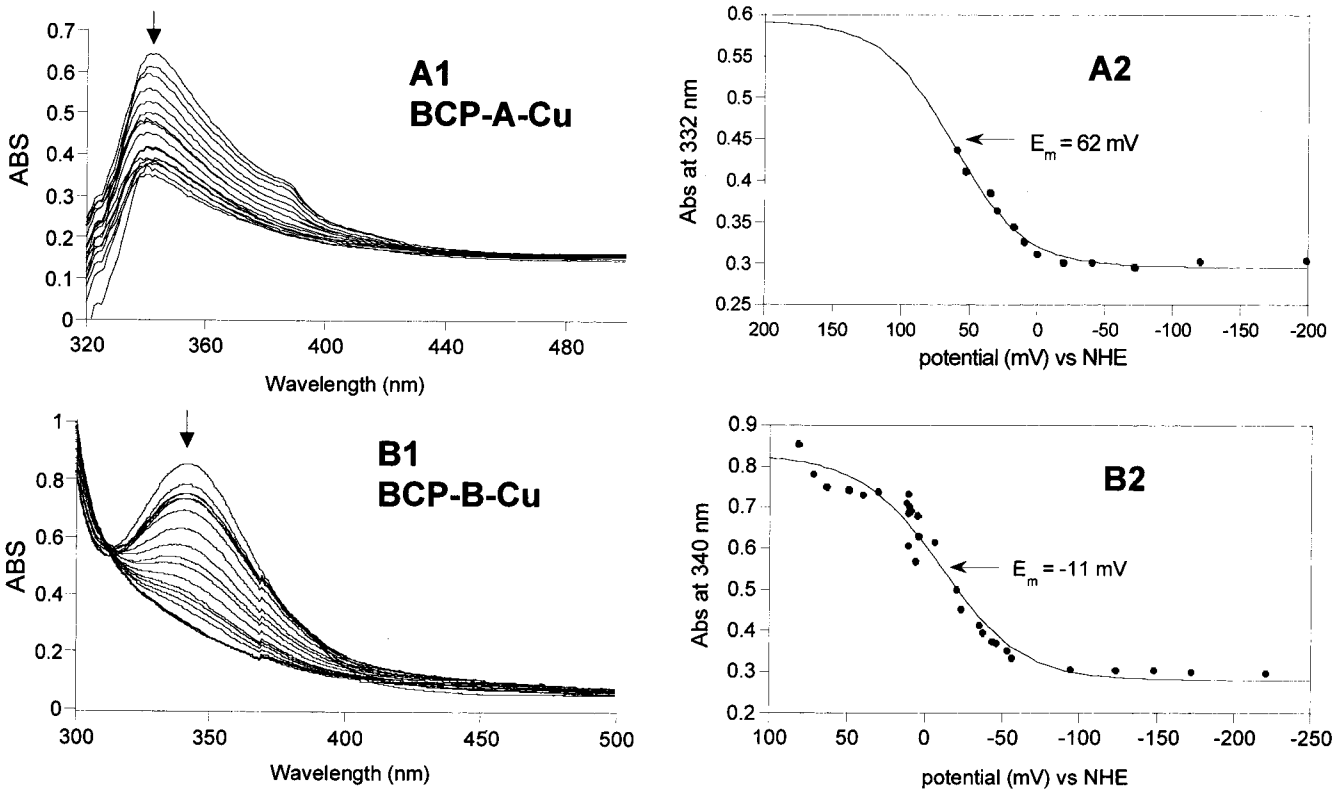

Figure 7. Potentiometry results for copper−peptide complexes. Representative UV−visible spectra following the reductions of (A1) BCP-A−Cu(II) and (B1) BCP-B−Cu(II). Absorbance at the LMCT band is plotted against the measured potential in mV vs NHE for (A2) BCP-A−Cu(II), LMCT = 332 nm, and (B2) BCP-B−Cu(II), LMCT = 340 nm. Data in filled circles are fit with the Nernst equation giving a midpoint potential E_m. One representative graph and fit are shown for each peptide−copper(II) complex.

point potential of the BCP-A−Cu(II) complex, resulting in the observation of only about half of the reduction curve. The difference in the reduction potentials of the BCP−Cu(II) complexes, which presumably have the same ligand set but different geometries, lends support to the possibility of a twist in the square plane for BCP-A−Cu(II) and not BCP-B−Cu(II).

Copper Complexes in Methanol. In an effort to exclude coordination of exogenous ligands, copper(II)−peptide complexes were formed in methanol using a procedure based on that reported by Vahrenkamp and co-workers for peptide−zinc(II) complexes,[43] which includes deprotonation of the peptide His and Cys ligands prior to addition of Cu(II). When deprotonation with $NaOCH_3$ preceded Cu(II) addition, BCP-A−Cu(II) and BCP-B−Cu(II) show S→Cu(II) LMCT bands at 410 and 360 nm ($\epsilon \sim 1400$ and 1700 M^{-1} cm^{-1}), respectively, and d−d bands around 600 and 560 nm (Supporting Information Figure S1). The red shift in the S→Cu(II) LMCT bands upon moving from aqueous to methanolic solution suggests that the less coordinating solvent allows some distortion toward tetrahedral geometries in both peptides.[32] Interestingly, the Cu(II) complex with BCP-A took >24 h to reach full yield, in methanol, while that of BCP-B was complete within 2−3 h. This may reflect a "preorganization" of the β-turn BCP-B peptide in methanolic solution. When complexes are prepared by direct addition of Cu(II) to the protonated peptide in methanol, in the absence of $NaOCH_3$, the LMCT bands shift to 430 nm for BCP-A−Cu(II) and 390 for BCP-B−Cu (Figure S1). The overall yield was less than half that obtained with deprotonation of the peptide prior to complex formation.

Co(II) Complexes and Metal−Peptide Stoichiometries. While Cu(II) complexes have significant ligand field stabilization energy (LFSE) in square-planar geometries, the differences in the LFSE for Co(II) in either octahedral or tetrahedral geometries are not as significant.[44] Both peptides bind Co(II) in a tetrahedral geometry with the Cys and His ligands, as evidenced by characteristic d−d bands at 625 nm with extinction coefficients of 230 and 290 M^{-1} cm^{-1} for Co(II)−BCP-A and Co(II)−BCP-B, respectively (Supporting Information Figure S2) and S→Co(II) LMCT bands at 310 nm with $\epsilon \sim 1100-1400$ M^{-1} cm^{-1}.[45−48] Upon inspection of the Co(II) titration curves for the complexes, however, the stoichiometry of peptide to metal binding was found to be 2:1 BCP:Co(II) for both complexes.

The peptide−metal stoichiometry was further investigated by analytical ultracentrifugation for both the Co(II) and Cu(II) BCP complexes.[49] The solution molecular weight

(43) Meibner, A.; Haehnel, W.; Vahrenkamp, H. *Chem. Eur. J.* **1997**, *3*, 261−267.
(44) Cotton, F. A.; Wilkinson, G.; Murillo, C. A.; Bochman, M. *Advanced Inorganic Chemistry*, 6th ed.; Wiley: New York, 1999.
(45) Bertini, I.; Luchinat, C. *Adv. Inorg. Chem.* **1984**, *6*, 71−111.
(46) Kaden, T. A.; Holmquist, B.; Vallee, B. L. *Inorg. Chem.* **1974**, *13*, 2585−2590.
(47) Klemba, M.; Regan, L. *Biochemistry* **1995**, *34*, 10094−10100.
(48) Guo, J.; Giedroc, D. P. *Biochemistry* **1997**, *36*, 730−742.
(49) Hensley, P. *Structure* **1996**, *4*, 367−373.

Table 2. Analytical Ultracentrifugation Parameters for Peptide Complexes with Cu(II) and Co(II)

sample	1:1 MW[a]	2:1 MW[a]	MW_{obs}[b]	stoichiometry[c]
BCP-A−Co(II)	2144	4231	8943	4:2
BCP-B−Co(II)	1496	2931	5189	4:2
BCP-B−Cu(II)	1500	2937	1522	1:1

[a] Expected molecular weight for given stoichiometry of peptide:metal complexes. [b] Observed solution molecular weight calculated from ultracentrifugation data. [c] Proposed peptide:metal stoichiometry based on MW_{obs}.

calculated from analytical ultracentrifugation monitored at the S→Co(II) LMCT band at 310 nm was approximately twice that of the expected molecular weight of the 2:1 complex, suggesting a tetrameric peptide complex binding two Co(II) ions (Table 2 and Supporting Information Figure S3). By contrast, the BCP-B−Cu(II) sample, monitored in the ultracentrifugation experiment at the 340 nm S→Cu(II) LMCT band, displayed a 1:1 Cu:peptide molecular weight (Supporting Information Figure S4).

The stoichiometry of the BCP−Cu(II) complexes was further investigated by preparing complexes of BCP−Cu(II) in separate samples with different concentrations of added Cu(II). For each sample the copper(II)−peptide complex was quantified by EPR spectroscopy, and the reduced Cys thiol assayed by Ellman's reagent (DTNB).[50] From these experiments, average BCP:Cu(II) ratios of 1.0 ± 0.3 for BCP-B−Cu(II) and 1.4 ± 0.3 for BCP-A−Cu(II) were determined. The stoichiometry results clearly indicate that although the Co(II)−BCP complexes are tetrameric with a 2:1 BCP to Co(II) stoichiometry, the BCP−Cu(II) complexes are monomeric with 1:1 BCP to Cu(II) concentrations.

Discussion

In this work we present the Cu(II) and Co(II) coordination properties of two peptides containing the blue copper ligand set of $His_2CysMet$. BCP-A incorporates the native plastocyanin ligand loop, whereas BCP-B is designed to bind metals with the plastocyanin ligand set. Both peptides form complexes with Cu(II) and Co(II) in aqueous solution and with Cu(II) in methanol solution, with properties summarized in Table 1. Stoichiometric (1:1) tetragonal Cu(II) complexes with SN_2X_n (X = solvent, $n = 1-3$) ligand environments are predicted for both of the Cu(II) peptide complexes (Figure 8) on the basis of S→Cu LMCT bands, EPR g and A values, and ENDOR spectra. For the cobalt(II)−peptide complexes, a tetrahedral geometry is evident from the Co(II) d−d band energy and extinction coefficients and is in contrast to the tetragonal geometry displayed for the complexes of these peptides with Cu(II). Interestingly, while the copper(II)−peptide complexes are monomeric, the Co(II) peptide complexes have an apparent 4:2 peptide:Co(II) ratio based on titration and analytical ultracentrifugation data.

The coordination properties of the two peptides indicate that both act as general metal-binding sites. One major hindrance to pseudo-tetrahedral binding in the BCP systems

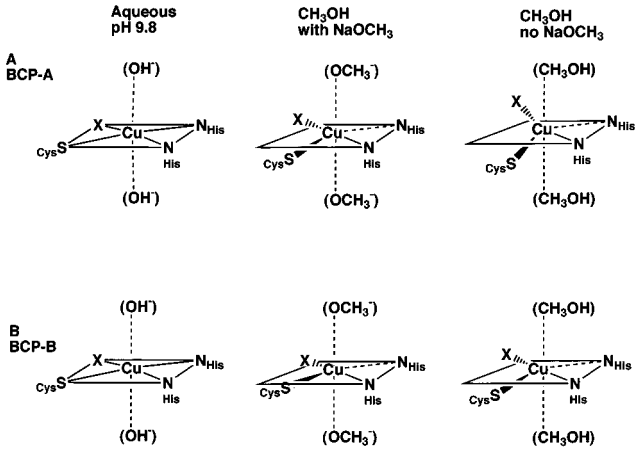

Figure 8. Proposed structures for (A) BCP-A−Cu(II) and (B) BCP-B−Cu(II) complexes in aqueous and methanolic solutions. Both complexes are predicted to exhibit slight tetrahedral distortions in methanol, and BCP-A−Cu(II) is predicted to have a higher degree of tetrahedral distortion than BCP-B−Cu(II).

is solvent accessibility to the Cu(II) binding site, which results in axial interactions of the solvent with the Cu(II) to form a stable Jahn−Teller or tetragonally distorted octahedral geometry.[44] In comparison with the simply designed BCP-B peptide, the plastocyanin Cu-binding loop in BCP-A seems to impart a tetrahedral distortion of the square plane onto the Cu(II), based upon the more intense d−d band, the larger shift of the LMCT band in methanol, and the more positive $E_{1/2}$ value. Even though this peptide is not sufficiently constrained to create a type 1 blue copper site in the absence of the protein, the ligand loop does distort the Cu(II) geometry toward that of the protein.

Accessibility of solvent or other protein ligands to the blue copper site is very important in the regulation of the reduction potential for the blue copper proteins. Figure 1 displays the effect of increased axial interaction of other protein ligands with the Cu(II) ion on the reduction potential of the blue copper protein. As axial ligands are added or strengthened, the reduction potential of the site becomes more negative, falling from ∼+800 mV vs NHE for laccases that have no axial interactions to ∼+180 mV for stellacyanin with a close axial O atom ligand. In stellacyanin, the oxygen ligand is donated from a Gln residue in the Met position (relative to plastocyanin or azurin). Amide oxygens are poorer ligands than H_2O, OH^-, CH_3OH, or NH_3, which are available for coordination in the BCP reaction mixtures. These stronger axial interactions in the BCP−Cu(II) complexes shift the redox potentials below the range of the blue copper sites. BCP-A−Cu(II), with the small twist in the square plane and stronger axial interactions than found in any native blue copper protein, has a reduction potential of +75 mV vs NHE showing that the site is poised between that of the native blue copper sites with more positive potential and the more negative reduction potential site in the BCP-B−Cu(II), which has no tetrahedral distortion, at −10 mV vs NHE.

Factors contributing to Cu(II/I) reduction potentials include type, geometry, and charge on the metal ligands. The peptide−copper(II) complexes described here show similarities to predictions from Cu(II) model chemistry, in which

(50) Riddles, P. W.; Blakekey, R. L.; Zerner, B. *Methods Enzymol.* **1983**, *91*, 49−61.

tetrahedral distortion and sulfur coordination both are expected to increase values of $E_{1/2}$. Comba has described the effect of tetrahedral distortion on the properties of a series of CuN_4 complexes.[51] A tetrahedral twist of 15° from the equatorial ligand square plane results in a 100 mV increase from −550 to −450 mV vs NHE in aqueous solution, similar to the increase observed for the more distorted BCP-A−Cu(II) complex. Of note, this distortion is not accompanied by a large decrease in the ^{63,65}Cu $A_{||}$ value in either model systems[51,52] or the peptide complexes. Substitution of sulfur for nitrogen ligands is expected to stabilize Cu(I), and is reflected in the more positive potentials measured here for the N_2SX (+ solvent) ligand set. These are more similar to square-pyramidal models with N_3S ligands, which have reported potentials of +62 to +80 mV (vs NHE in aqueous solution), and also show sensitivity to tetrahedral distortion.[53] In addition to geometry, charge neutralization by solvent-derived ligands is likely playing a role in the relatively low potentials observed for the BCP−CU(II) complexes relative to the native proteins.

It is of interest to compare the BCP−Cu(II) complexes with the unfolded state of plastocyanin or azurin. In thermal denaturation studies of either plastocyanin or azurin, protein unfolding has been accompanied by the loss of sulfur coordination to the Cu(II), observed with loss of the S→Cu LMCT band or by the change of the EPR spectrum to one similar to a type 2 site without sulfur coordination.[54,55] All cases of thermal denaturation are irreversible, suggesting a change in the protein or Cu(II), such as oxidation of the Cys thiol, that hinders reformation of a type 1 site. In none of the above studies were steps taken to control potential redox chemistry between the Cu(II) and Cys, however. The results presented here indicate that the plastocyanin loop sequence in the BCP-A−Cu(II) complex, unconstrained by the rest of the folded protein, is able to provide the Cys and His ligands for complexation. This suggests that the ligand loop should serve as a metal-binding site in the unfolded protein at ambient temperature.

Indeed, when azurin is unfolded with high concentrations of guanidinium hydrochloride instead of thermally, the Cu(II) ion initially remains bound to the ligand loop His and Cys, but the redox process between Cu(II) and Cys occurs slowly over time.[56] The reduction potential of GuHCl-unfolded azurin was measured to be +456 mV vs NHE,[57] about 130 mV more positive than the reduction potential for folded azurin at +320 mV, indicating that Cu(I) is stabilized in this particular unfolded state. The coordination environment of Cu(I) in unfolded azurin has been investigated by EXAFS[58] and modeled to consist of Cys, one His, and potentially a chloride ion, suggesting as found here that the Cu binding loop contributes ligands in the absence of the surrounding folded protein. From the studies with BCP-A, however, it is clear that a solvent-exposed complex would gain additional axial ligands. This suggests that in the unfolded state of azurin, the Cu ion is not fully solvent accessible.

Summary

In an effort to enhance understanding of the biophysical interactions that stabilize the blue copper site, we have characterized the coordination properties of two peptides containing either the ligand loop of plastocyanin or the ligand set from plastocyanin. These initial designs for the blue copper peptides (BCP's) were found to bind Cu(II) through histidine and cysteine ligands. The BCP−Cu(II) complexes were spectroscopically characterized and determined to have tetragonal geometries and additional solvent ligands, with a twist in the square plane of the ligand loop peptide BCP-A−Cu(II) complex. This distortion is accompanied by an increase of the Cu(II/I) reduction potential. From the results presented here and of the blue copper design studies thus far, it is obvious that the protein matrix, not just the ligands and immediate secondary interactions, plays a large role in shielding the Cu(II/I) site from solvent and keeping the cysteine unavailable for disulfide formation. The ability demonstrated here to at least partially control the Cu(II)−Cys redox chemistry has allowed the synthesis of well-characterized Cu(II) peptide complexes with Cu(II)−Cys thiolate bonds, laying the groundwork for future design efforts.

Materials and Methods

Peptide Design. Peptides were designed on the basis of the crystal structure and sequence of Poplar plastocyanin (1PLC)[10] pictured in Figure 2. Molecular modeling and energy minimizations for apopeptides (sequences in Figure 3) were performed with the Amber force field[59] in the Insight II molecular simulations package (MSI) with no solvent interactions. Peptides were built as linear models and subjected to energy minimization using molecular mechanics; energy-minimized structures were altered manually and reminimized to check for converged structures, suggesting global vs local energy minima. Criteria for "successful" design were optimized structures predicted to have all four metal ligands in proximity with no other obvious steric hindrances for metal coordination.

Peptide Synthesis and Purification. Peptides were synthesized at a 0.2 mmol scale on a continuous flow PerSeptive Biosystems Pioneer Solid Phase synthesizer (Framingham, MA). The OH− amino acids were FMOC protected at the amine, *tert*-butyl protected at hydroxyl and carboxyl side chains, and trityl protected at His

(51) Comba, P. *Coord. Chem. Rev.* **1999**, *182*, 343−371.
(52) Comba, P.; Hambley, T. W.; Hitchman, M. A.; Stratemeier, H. *Inorg. Chem.* **1995**, *34*, 3903−3911.
(53) Ambundo, E. A.; Deydier, M.-V.; Grall, A. J.; Aguera-Vega, N.; Dressel, L. T.; Cooper, T. H.; Heeg, M. J.; Ochrymowycz, L. A.; Rorabacher, D. B. *Inorg. Chem.* **1999**, *38*, 4233−4242.
(54) (a) LaRosa, C.; Milardi, D.; Grasso, D.; Guzzi, R.; Sportelli, L. *J. Phys. Chem.* **1995**, *99*, 1864−14870. (b) Milardi, D.; LaRosa, C.; Grasso, D.; Guzzi, R.; Sportelli, L.; Fini, C. *Eur. Biophys. J.* **1998**, *27*, 273−282.
(55) Guzzi, R.; Sportelli, L.; LaRosa, C.; Milardi, D.; Grasso, D.; Verbeet, M. P.; Canters, G. W. *Biophys. J.* **1999**, *77*, 1052−1063.
(56) Leckner, J.; Wittung, P.; Bonander, N.; Karlsson, B. G.; Malström, B. G. *J. Biol. Inorg. Chem.* **1997**, *2*, 368−371.
(57) Wittung-Stafshede, P.; Hill, M. G.; Gomez, E.; DiBilio, A.; Karlsson, B. G.; Leckner, J.; Winkler, J. R.; Gray, H. B.; Malström, B. G. *J. Biol. Inorg. Chem.* **1998**, *3*, 367−370.
(58) DeBeer, S.; Wittung-Stafshede, P.; Leckner, J.; Karlsson, G.; Winkler, J. R.; Gray, H. B.; Malström, B. G.; Solomon, I.; Hedman, B.; Hodgson, K. O. *Inorg. Chim. Acta* **2000**, *297*, 278−282.
(59) Kini, R. M.; Evans, H. J. *J. Biomol. Struct. Dyn.* **1991**, *9*, 475−488.

and Cys side chains. PAL-PEG-PS resin (PerSeptive) was used as the solid-phase support for single amino acid standard coupling cycles employing the HBTU (2-(1*H*−benzotriazole-1-yl)-1,1,3,3-tetramethyluronium hexafluorophosphate) and HOBT (*N*−hydroxybenzotriazole·H_2O) activator combination. After completion of the automated peptide assembly, the resin-bound peptide was washed with *N*,*N*-dimethylformamide (DMF), isopropyl alcohol, and dichloromethane consecutively. The peptides were acylated on the N-terminus with a mixture of 50 (v/v):50 acetic anhydride:pyridine, which reacted for 1 h. Prior to cleavage, the resin was thoroughly washed as above. The cleavage reagent (20 mL), composed of 90% (v/v) trifluoroacetic acid (TFA), 8% ethanedithiol, and 2% water, was added to the resin and allowed to react for at least 1 h, or until the resultant peptide appeared fully deprotected by analytical HPLC. The cleavage mixture, now containing the cleaved peptide, was drained from the resin and evaporated to near dryness. The crude peptide was precipitated with cold ether, suspended in 0.1% (v/v) aqueous TFA, and lyophilized. Purification of crude peptide was accomplished by reverse-phase C18 HPLC using a water−acetonitrile (Fisher, HPLC grade) solvent system containing 0.1% (v/v) TFA. Peptide identities were confirmed by MALDI mass spectrometry observing the molecular ion peak. Peptide concentrations were determined by UV−vis spectroscopy at 280 nm ($\epsilon_{BCP-A} = 6690\ M^{-1}\ cm^{-1}$; $\epsilon_{BCP-B} = 5560\ M^{-1}\ cm^{-1}$). All chemicals and solvents used for peptide synthesis were of high purity (sequencing grade) and purchased from either Aldrich or Fisher. Unless noted otherwise all other chemicals were reagent grade.

Peptide−Copper Complexes in Aqueous Solution. Purified, lyophilized peptide was taken into the N_2 glovebox, where it was dissolved into an aqueous pH 9.8 buffer composed of 50 mM boric acid, 10 mM HEPES, 50 mM NH_4OH, and 50 mM KCl.[31] The concentration of total peptide was quantified by UV−vis absorption at 280 nm, and the percentage of reduced peptide was determined by reaction of the peptide with 5 mM 5,5′-dithiobis(2-nitrobenzoic acid) (DTNB; Aldrich) in pH = 7.3 phosphate buffer containing 1 mM EDTA using $\epsilon_{412} = 14\ 100$ per DTNB-modified thiol.[50]

A 1 equiv amount of $CuSO_4$ was added from a stock solution of 50 mM $CuSO_4$ in H_2O. Upon addition of Cu(II), the solution turned a light violet color, more visible for BCP-A than BCP-B. After mixing with slight agitation, the solution was placed in a septum-sealed cuvette for absorption measurements. After several hours, the BCP-A and BCP-B solutions showed an orange/brown precipitate, most likely due to reduction and decomposition of the sample.

EPR and ENDOR. EPR and ENDOR samples were prepared under nitrogen or argon atmosphere. X-band EPR measurements were performed at 10 K using a Bruker ESP-300E spectrometer. Q-band (34 GHz) EPR and ENDOR spectra were recorded on a home-built Q-band EPR spectrometer.[60] Quartz tubes (2.0 mm i.d., 2.4 mm o.d.; Wilmad Glass) were used for all ENDOR samples. Samples of BCP-A−Cu(II) required addition of 25% glycerol for cryoprotection.

Quantitation of Cu(II):BCP Ratios. Samples of BCP-B−Cu(II) were prepared with 1.0, 1.5, 2.0, and 2.5 equiv of Cu(II) added to separate BCP-B samples. After complex formation, the [BCP-S^-] was quantified by reaction with DTNB. EPR spectra were acquired, and the signal from any excess buffer-coordinated Cu(II) was subtracted from the EPR spectrum of each sample. The [Cu(II)] giving rise to the BCP-B−Cu(II) EPR signal was quantified by comparison of the normalized double integral with that of 0.5 mM Cu(II)EDTA. EPR samples of BCP-A−Cu(II) were not stable without the presence of cryoprotectant. Two 1:1 BCP-A:Cu(II) samples were prepared with either 15 or 25% glycerol as cryoprotectant. Each sample was reacted with DTNB to quantitate the [BCP-S^-], and the normalized double integral was used to quantitate [Cu(II)]. At 25% glycerol, the concentration of [BCP-S^-] was based upon the average value of ϵ_{LMCT} and ϵ_{d-d} established with approximately 10 different sample preparations.

Redox Potentiometry. Redox titrations were performed in combination with electronic spectroscopy, using a Cary UV−visible spectrophotometer. BCP-A−Cu(II) or BCP-B−Cu(II) samples were prepared under N_2 atmosphere in a glovebox. The sample was placed in a septum-sealed container, removed from the glovebox, and added to the in-house designed glass redox cuvette with a syringe. The solution potentials were measured under N_2 flow with platinum measuring and calomel reference electrodes (Radiometer Analytical, Lyon, France) standardized against freshly prepared quinhydrone (Aldrich) in pH 7 phosphate buffer solution, + 47 mV vs SCE. All potentials were measured vs SCE and converted to NHE by the addition of +244 mV. Initial spectra and potential readings were taken upon adding the peptide solution to the redox cuvette. After stabilization, the potential of the solution was adjusted to more negative values using 1−3 μL aliquots of freshly prepared sodium dithionite (Aldrich) in pH 7.5 phosphate buffer. Once the sample was fully reduced, evidenced by the loss of the S→Cu(II) LMCT band, and no further change upon addition of dithionite, the potential was adjusted to more positive potentials with 1 μL aliquots of potassium ferricyanide in pH 7.5 buffer. The following redox mediators were taken from 2 mM stock solutions in DMSO and diluted to 2 μM final concentration to stabilize the solution reduction potential: duroquinone, 2-hydroxy-1,4-naphthoquinone, 5-hydroxy-1,4-naphthoquinone, anthraquinone-2-sulfonate, anthraquinone-2,6-sulfonate, benzyl viologen, methyl viologen, 1,4-naphthoquinone, 1,2-naphthoquinone, 1,4-naphthoquinone-2-sulfonate, 2,6-dimethylbenzoquinone, methyl-1,4-benzoquinone, and phenazine methosulfate, with E_m's in the range of +175 to −430 mV vs NHE or −69 mV to −674 mV vs SCE. Upon completion of the titration, the absorbance intensity at λ_{max} was plotted versus the measured potential. The resulting curve was fit to the Nernst equation

$$Y = A_{red} + \Delta A\left[\frac{1}{(10^{nF(E_h - E_m/RT)} + 1)}\right]$$

where A_{red} is the absorbance at full reduction, ΔA is the change in absorbance from oxidized to reduced, E_h is the measured potential, and E_m is the reduction midpoint potential.[61] The number of electrons, n, was set to 1, while A_{red}, ΔA, and E_m were allowed to vary in the nonlinear fit. All reduction potentials reported are versus NHE.

Peptide−Copper Complexes in Methanol. Peptide reactions in methanol were performed under nitrogen atmosphere using Schlenk techniques and a nitrogen filled glovebag. Methanol (EM Science, reagent grade) was dried over magnesium iodide and distilled under nitrogen. UV−vis absorption spectra for methanol reactions were recorded on a Milton Roy diode array spectrophotometer in 100 μL cuvettes with airtight Teflon caps.

Methoxide Deprotonation. To a 1−2 mM solution of BCP-A or BCP-B in methanol, 3 equiv of sodium methoxide (Aldrich, 95%) solution in methanol was added dropwise by syringe to a septum

(60) Morrissey, S. R.; Horton, T. E.; DeRose, V. J. *J. Am. Chem. Soc.* **2000**, *122*, 3473−3481.

(61) Shifman, J. M.; Gibney, B. R.; Sharp, R. E.; Dutton, P. L. *Biochemistry* **2000**, *39*, 14813−14821.

sealed flask.[43] The solution was allowed to stir at 45 °C for 4 h. A 1 equiv amount of $Cu(NO_3)_2 \cdot 2.5H_2O$ (Aldrich) in methanol was then added and allowed to stir for an additional 1 h at 40 °C. Heat was removed, and the solutions were allowed to stir until the reaction was completed. The solution was then centrifuged to remove any precipitate. BCP-A−Cu(II) required several hours (>24) to fully form a complex, indicated by no more change in the absorption spectrum. BCP-B−Cu(II) was fully formed in 2−3 h.

No Deprotonation. To a 1.1−1.6 mM solution of BCP-A or BCP-B in methanol, 1 equiv of $Cu(NO_3)_2 \cdot 2.5H_2O$ in methanol was added dropwise with stirring. The solution was allowed to stir at 45 °C for 4 h. After 4 h, the heat was reduced to 35 °C, and the solution was allowed to stir for 12 h more. After 12 h, the solution was placed in an ice bath to cool. Precipitate was removed by centrifugation, and the solution was eluted through a Sephadex-LH 20 gel filtration column (Amersham Pharmacia Biotech). The total peptide concentration in each elution was quantified using A_{280}, and the percentage of reduced peptide was determined by DTNB assay.

Cobalt Titrations. Dried peptide was dissolved in 25 mM HEPES (EM Science, Omnipur) at pH 7.5 under argon atmosphere. The total and reduced peptide concentrations were quantified with the absorbance at 280 nm and the DTNB assay as described for the Cu(II) complexes. The peptide solution was placed in a double septum sealed anaerobic cuvette and titrated by addition of $CoCl_2$ (Alfa Aeser, Puratronic), quantified by flame atomic absorption spectroscopy, from a gastight syringe. The spectra were recorded on a Hewlett-Packard 8452A spectrophotometer. At the end of the titration the amount of reduced peptide was requantified with the DTNB assay.

For each titration point the spectrum of cobalt(II)−peptide was corrected for dilution, and the spectrum of the apopeptide was subtracted. A plot of absorption (A) as a function of the total [Co^{2+}] is used to determine the stoichiometry of the Co(II)−BCP complex.

Analytical Ultracentrifugation. Co(II) and Cu(II)-peptide samples for analytical ultracentrifugation were prepared as described above. Co(II)−BCP complexes, BCP-B−Cu(II), and apopeptide BCP-B were prepared in sufficient concentration to have an approximate absorbance of 0.5 au at the LMCT band wavelength for the metal−BCP complexes or at 280 nm for the apo-BCP-B. All samples were prepared in an MBraun glovebox under N_2 atmosphere. The samples were loaded into six-slotted sample holders for analytical ultracentrifugation (Beckman), where one row of three slots contained samples and the other row contained the buffer reference. The sample holders were assembled in the glovebox and then removed for the experiment. The samples were spun at 48 000 rpm for 16−24 h, or until equilibrium was reached at 4 °C under vacuum. The absorbance at 280, 303, and either 330 or 340 nm was taken at several radial points along the sample cell every 4 h. The data, absorbance vs a function of radial position was edited with "WinREEDIT" and fit with "WinNONLIN,"[62] both shareware programs available from Dr. John Philo's software homepage for ultracentrifugation, http://www.jphilo.mailway.com, at The National Analytical Ultracentrifugation Facility of the University of Connecticut Biotechnology Center. "SEDENTERP" was used to calculate the molecular weight from the "WinNONLIN" fit parameter, σ.[49]

Acknowledgment. We are grateful for the use of equipment in the research laboratories of P. A. Lindahl and D. P. Giedroc at Texas A&M University. This work is supported by the Robert A. Welch Foundation (V.J.D.), the NIH (Training Grant BM08523, R.G.D.), and the Texas A&M University WFN (R.G.D.). EPR facilities and molecular modeling facilities at Texas A&M are supported by the NSF (Grants CHE-8912763 and CHE-9528196, respectively). V.J.D. is a Cottrell Scholar of the Research Corporation.

Supporting Information Available: UV−visible spectra of BCP−Cu(II) complexes in methanol solution, UV−visible spectra and titration curves for aqueous Co(II)−BCP complexes, and analytical ultracentrifugation data for Co(II)−BCP and BCP-B−Cu(II) complexes. This material is available free of charge via the Internet at http://pubs.acs.org.

IC010555A

(62) Johnson, M. L.; Correia, J. J.; Yphantis, D. A.; Halvorson, H. R. *Biophys. J.* **1981**, *36*, 575−585.